Int. J. Nanosci. Nanotechnol., Vol. 11, No. 2, June 2015, pp. 115-122

Effect of Nitric acid on Particle Morphology of the Nano-TiO_2

M. Ramazani, M. Farahmandjou* and T.P. Firoozabadi

Department of Physics, Varamin Pishva Branch, Islamis Azad University, Varamin, I. R. Iran

(*) Corresponding author: farahmandjou@iauvaramin.ac.ir
(Received: 19 Dec 2014 and Accepted: 31 May. 2015)

Abstract
Nano-sized titanium dioxide TiO_2 powder was prepared by new wet chemical route from its precursor Titanium (IV) chloride ($TiCl_4$) as precursor with isopropoxy alcohol in presence of nitric acid under ambient condition. Their morphologies, phase compositions and components of the TiO_2 nanoparticles were characterized by transmission electron microscopy (TEM), field emission scanning electron microscopy (FE-SEM), X-ray diffraction (XRD), electron dispersive spectroscopy (EDS), Fourier transform infrared spectroscopy (FTIR) and UV-Vis spectrophotometer. The TEM results showed the as-synthesized TiO_2 formed in nanometer scale. The FE-SEM images showed that the size of TiO_2 nanoparicles decreased with increasing annealing temperature while the uniformity of size distribution decreased. The FE-SEM images also revealed that the size of annealed TiO_2 nanocrystals increased with increasing the value of nitric acid. The average grain size of anatase nanoparticles was obtained about 25nm. The crystal structure of the nanoparticles before and after annealing was analyzed by XRD analysis. When the calcinations increased above 550^oC, the phase transformation of anatase to rutile occurred, but the anatase phase was still dominant. The sharp peaks in FTIR spectrum determined the purity of TiO_2 nanoparticles and absorbance peak of UV-Vis spectrum showed anatase phase at wavelength about 380 nm with band gap of 3.26 ev for as-prepared TiO_2 and rutile phase at wavelength about 382 nm with band gap of 3.24 ev for annealed TiO_2 nanoparticles. The EDS spectrum showed peaks of titanium and oxygen.
Keywords*: Nano-TiO_2, Wet chemical, Synthesis, Phase transition, Anatase phase.*

1. INRODUCTION

Highly ordered titania nanostructures of nanometer periodicity are very promising materials due to their specifically size-related properties. TiO_2 has been considerably investigated and utilized in a wide range of applications because of their useful electrical and optical properties, such as high dielectric constant [1], high electrical resistivity, high refractive index, excellent optical transmittance in the visible range [2], non-toxicity, large band gap, photocatalysts, gas sensors, photovoltaics and lithium ion batteries [3]. TiO_2 has three main crystalline structures: anatase (tetragonal-4/*mmm*) space group: $P4_1/amd$-D^{19}_{4h}, brookite (orthorhombic-*mmm*), pbca-D^{15}_{2h} and rutile (tetragonal-4/*mmm*), $P4_2/mnm$-D^{14}_{4h}. Rutile is usually stable at high temperatures. Different structures lead to different physical properties which in turn lead to different applications. [4]**.** Titanium dioxide of both anatase and rutile phases are usually found in industrial applications. Anatase is a useful catalyst in photochemistry because of its high photoactivity and rutile is a common white pigment being employed for its superior optical hiding power.

It is also well known that TiO_2 is one of the most superior semiconductor materials for decomposing organic materials due to its strong photocatalytic property. TiO_2 semiconductor becomes a photocatalyst when exposed to ultraviolet or near-visible light ($E \geq E$ band gap) with wavelengths shorter than 390 nm. If this light is absorbed by the semiconductor surface, it will have enough energy to overcome the energy barrier and excite an electron to transfer the electron from the filled valence band (VB) to the empty conduction band (CB), leaving an electron deficiency (hole) in the valence band. Once the charge carriers are generated across the band gap, they may transfer to the semiconductor surface and be absorbed by the reactants. The generation of charge carrier (electron-hole pairs) leads to the formation of highly oxidizing hydroxyl and superoxide radicals. These two species are capable of oxidizing practically all organic materials [5]. TiO_2 nanoparticles have been synthesized using various methods such as hydrothermal, sonochemical, solvothermal, reverse micelles, and sol gel reaction [6-15] for those applications. Wet chemical method has novel features which are of considerable interest due to its low cost, easy preparation, uniform size, unagglomerated state, high purity and homogeneous nanoparticles and industrial viability. Anatase phase is commonly obtained by hydrolysis of titanium compounds, such as titanium tetrachloride ($TiCl_4$) [16] or titanium alkoxides ($Ti(OR)_4$), in solution [17]. In the present work, anatase and rutile phases of TiO_2 nanoparticles are synthesized by wet chemical route and just combine $TiCl_4$ as a precursor in presence of nitric acid. The novelty of this work is the investigation of the effect of nitric acid on the size and morphology of the TiO_2 nanoparticles. The structural and optical properties of TiO_2 have been studied by XRD, EDS, TEM, FE-SEM, FTIR and UV-visible analyses.

2. EXPERIMENTAL DETAIL

5mL $TiCl_4$ (99.5% Merck) was slowly added dropwise into aqueous mixed solutions of 15 mL 2-isopropoxyethanol (99.6% Merck) and 150 mL deionized water under stiring at room temperature. A large amount of HCl gas was exhausted during the mixing process and then milk-like white solution was obtained. After that 2mL nitric acid was added to the solution and temperature was then increased to 90^0C for 1 hour. The pH was determined after adding nitric acid in the range for 0.5 to 1. In order to more morphological investigation the value of nitric acid was changed between 0-10mL.

The product was then aged at 220^oC for 2.5 hours without any washing and purification in opposite to other preparation methods [18] and finally calcined at different temperature in the range of 220 to 1000^oC for 3 hours. The white TiO_2 powder was later obtained. The morphologies of the samples were obtained by field emission scanning electron microscopy (FE-SEM) with type KYKY-EM3200, 25kV. Transmission electron microscopy (TEM) images were obtained on a Zeiss EM-900 microscope using an accelerator voltage of 80kV. X-ray diffractometer (XRD) was used to identify the crystalline phase and to estimate the crystalline size with 2θ in the range of 4-85^o with type X-Pert Pro MPD Cu-K_α: $\lambda = 1.54$Å. The optical properties of absorption were acquired by ultraviolet–visible spectrophotometer (UV–Vis) with optima SP-300 plus, and Fourier transform infrared spectroscopy (FTIR) with WQF 510. The Ti and O elemental analysis of the samples was performed by energy dispersive spectroscopy (EDS) type VEGA, 15kV. All the measurements were carried out at room temperature.

3. RESULTS AND DISCUSSION

Figure.1 shows the XRD pattern of the nanoparticles annealed at different temperature. Fig. 1(a) shows the as-synthesized TiO_2 nanoparticles which indicate the structure of tetragonal anatase

phase. The XRD patterns showed this sample have four sharp peaks 2θ angle with the peak position at 25.2°, 37.7 °, 47.8 °, 54.1 °, 62.5 °, 69.4 ° and 75.5° with (101), (004), (200) , (105), (204), (116) and (215) diffraction planes, respectively which are in accordance with the TiO_2 anatase phase. Fig. 1(b) shows the annealed TiO_2 at 500°C in absence of nitric acid and Figure. 1(c) shows the annealed TiO_2 at 550°C in presence of nitric acid and Figure. 1(d) shows the annealed TiO_2 at 1000°C. It can be seen when the calcinations increased in the region after 500°C, the phase transformation from anatase to rutile occurred in TiO_2 nanopowders, but anatase phase was still dominant. It can be seen the peak position at 27.5° corresponds to the plane (110) of rutile form. The rutile structure for annealed nanocrystals was obtained at 1000°C. The mean size of the ordered TiO_2 nanoparticles has been estimated from full width at half maximum (FWHM) and Debye-Sherrer formula according to the following equation:

$$D = \frac{0.89\lambda}{B\cos\theta} \qquad (1)$$

where, 0.89 is the shape factor, λ is the x-ray wavelength, B is the line broadening at half the maximum intensity (FWHM) in radians, and θ is the Bragg angle. The mean size of as-prepared TiO_2 nanoparticles was 25 nm from Debye-Sherrer equation.

Energy dispersive spectroscopy (EDS) of TiO2 prepared by wet synthesis method is shown in Figure. 2 which confirms the existence of Ti and O with weight percent. EDS was used to analyze the chemical composition of a material under FE-SEM. EDS shows peaks of titanium and oxygen and indicates fewer impurities such as chlorine in prepared TiO2.

Figure.3 presents FE-SEM images of TiO_2 nanoparticle. The morphology of nanoparticles varied with temperature. Fig. 3(a) shows the FE-SEM images of the as-prepared TiO_2 nanoparticles prepared by wet chemical method. In this figure, spherical TiO_2 nanoparticles are observed in the size range of 24-32nm. Figure. 3(b) shows the FE-SEM images of the annealed TiO_2 nanoparticles at 550°C for 3 hours. The TiO_2 nanoparticles formed were not agglomerated and average grange size of the smallest nanoparticles decreased to 12nm.

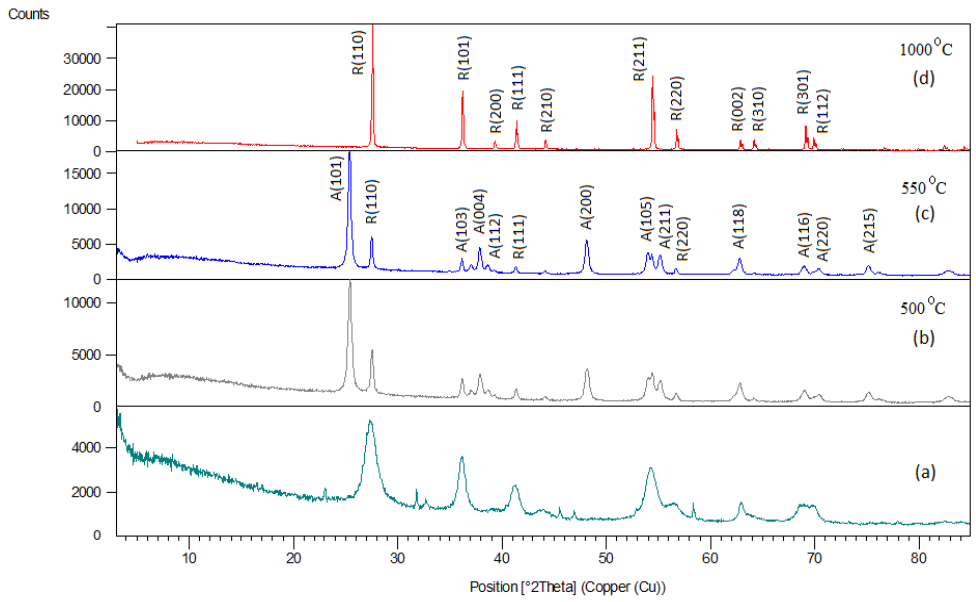

Figure 1. *XRD pattern of TiO_2 nanoparticles (a) as-synthesized; (b) annealed at 500°C; (c) 550°C and (d) 1000°C.*

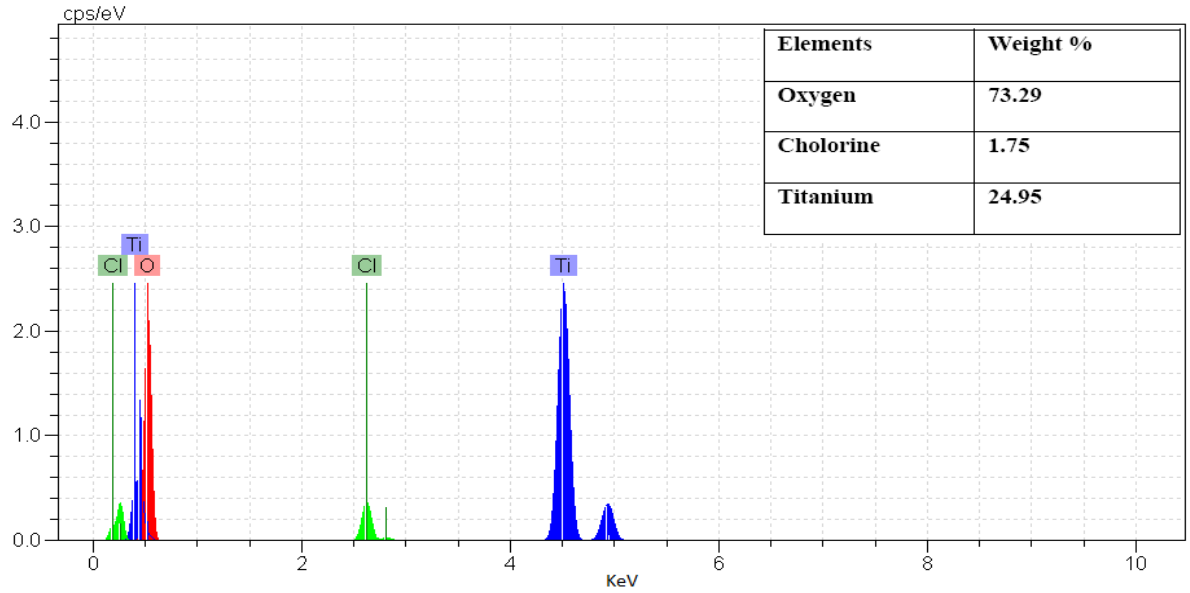

***Figure 2**. EDS spectra of the as-synthesized TiO2 prepared by wet synthesis*

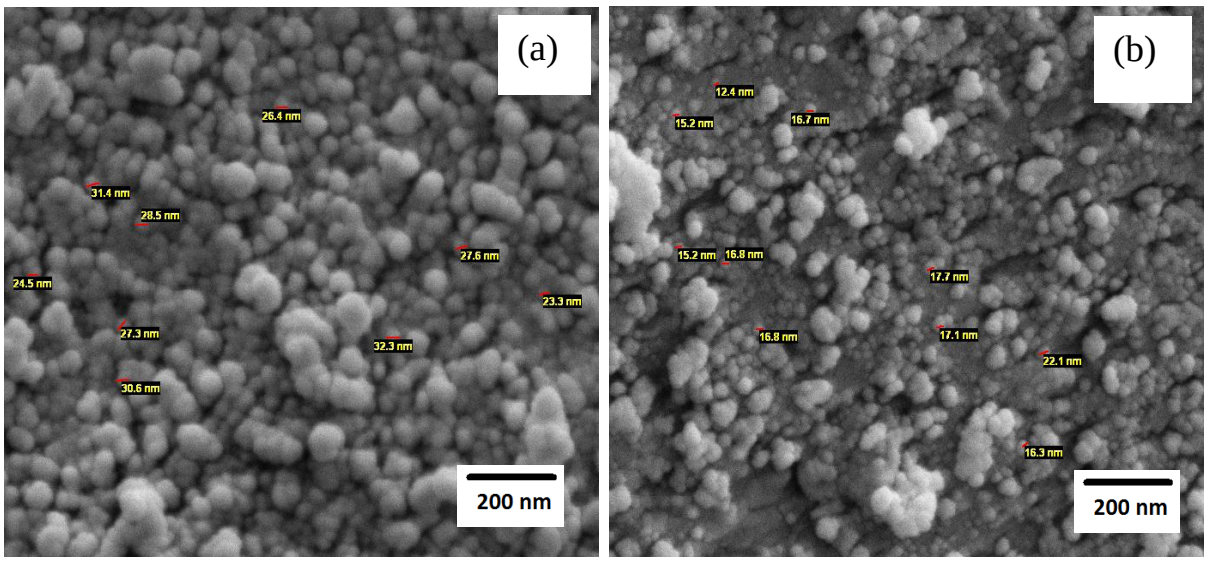

***Figure 3**. FE-SEM images of the TiO_2 (a) as-prepared (b) annealed at 550^oC.*

In Figure 4 the effect of nitric acid of the morphology of the TiO_2 nanoparticles has been studied. In Figure. 4(a) the samples were prepared without nitric acid and in Fig. 4(b) the samples were prepared with 2 mL nitric acid and in Figure. 4(c) the samples were prepared with 10 mL nitric acid. It can be seen from FE-SEM images that the size of annealed TiO_2 nanocrystals increases with increasing the value of nitric acid from 0-10mL. When the value of nitric acid is adjusted to 2 mL, the uniformity of the size with clumped distributions is visible through the FE-SEM analysis.

TEM was used for further examination of the morphology of the particles. Fig. 4 shows the as-synthesized TEM image of titanium dioxide prepared by wet synthesis. It is observed that the anatase TiO_2 nanoparticles with average particle size about 25nm are formed. The principal novelty of the procedure developed is the synthesis of TiO_2 nanoparticles with a regular distribution, uniform size and spherical shape.

According to Fig. 5, the infrared spectrum (FTIR) of the synthesized TiO_2 nanoparticles was in the range of 400-

4000cm^{-1} wave number which identifies the chemical bonds as well as functional groups in the compound. The large broad band at 3415cm^{-1} and 3146cm^{-1} is due to the OH stretching. These bands correspond to O-H vibration of the Ti-OH group and H_2O molecules. The sharp bands at 1383cm^{-1} can be assigned to the bending mode of nitrate group as a result of nitric acid addition. The low energy region and large broad band (below 1000cm^{-1}) at 621cm^{-1} indicates the stretching mode of Ti-O bond of a TiO_2 network. This bond is an important functional group that is related to the photocatalytic activity.

Absorbance peak of UV-Vis spectrum showed anatase phase at wavelength about 380nm with band gap about 3.26ev for as-prepared TiO_2 and rutile phase at wavelength about 382nm with band gap about 3.24ev for annealed TiO_2 nanoparticles. UV–Vis absorption spectra of as-prepared and annealed TiO_2 nanoparticles are shown in Figure. 6. For as-synthesized TiO_2 nanoparticles, the strong absorption band at low wavelength near 380 nm for anatase related to the band gap about 3.26ev (Figure. 6(a)) and for annealed TiO_2 nanoparticles the strong absorption band at low wavelength near 382 nm for rutile phase related to band gap about 3.24ev (Figure. 6(b)) indicate the presence of phase transition of anatase to rutile for TiO_2 nanoparticles under heat treatment at 600^{o}C.

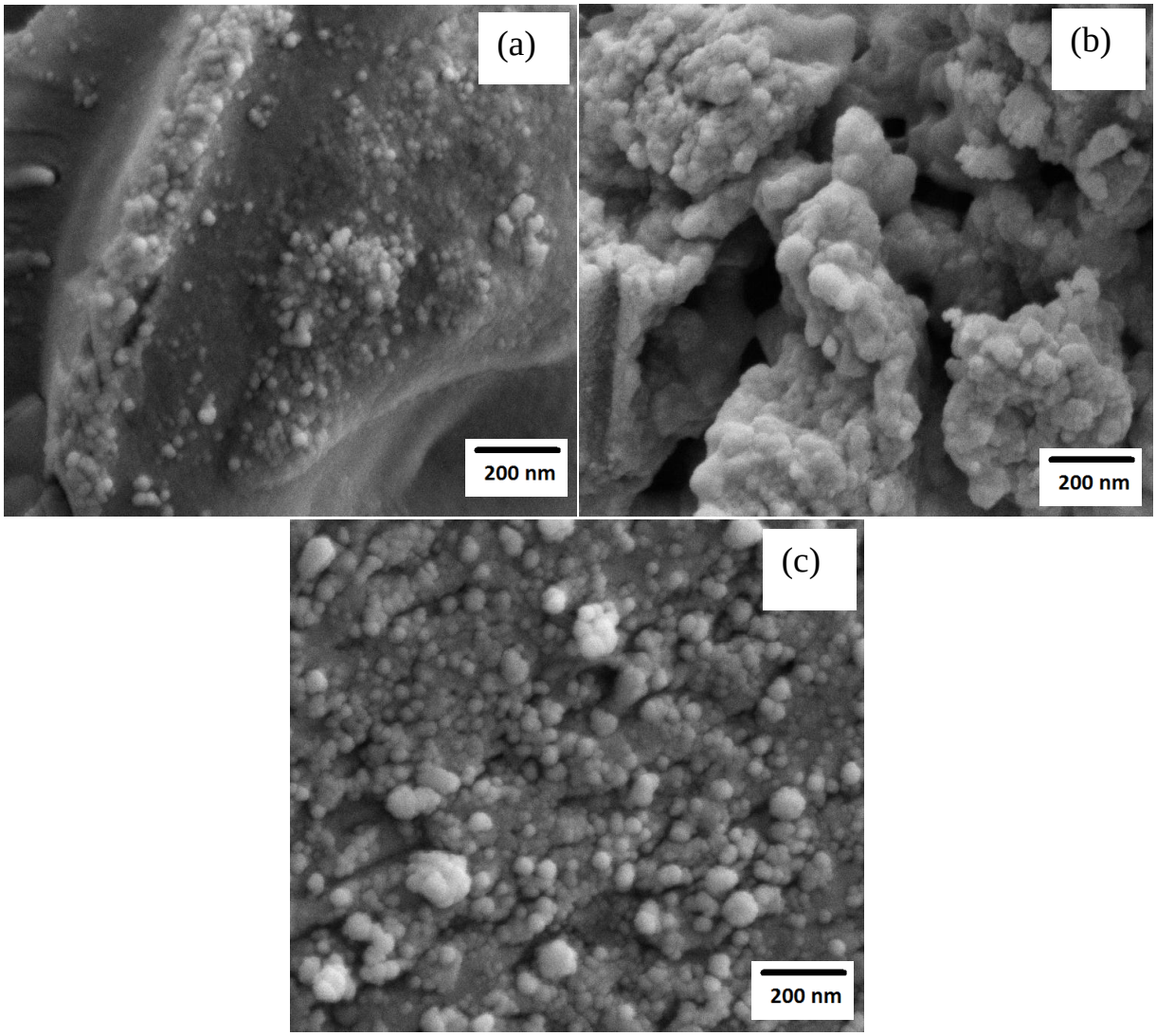

Figure 4. *FE-SEM images of TiO_2 nanoparticles: (a) samples without nitric acid; (b) with 2mL and (c) with 10mL.*

The absorption edge extends to longer wavelengths for TiO_2 nanoparticles, and absorption tail in the visible-light region over 350–500nm [19] and strong absorption band in the UV-light region are clearly observed.

4. CONCLUSION

Nano-TiO_2 was successfully prepared by simple and new wet synthesis method. Anatase to rutile phase transformation was achieved by calcinations more than 550^{o}C. TEM studies showed spherical structure of TiO_2 nanoparticles with mean particle size of 25nm. FE-SEM images showed that with increasing temperature the size of unagglomerate spherical naoparticles decreased to 12nm with uniformity of the size but the distribution of the size of nanoparticles increased. EDS showed the absence of impurities in prepared TiO_2. XRD pattern of TiO_2 nanoparticles demonstrated that the phase transition from anatas to rutile was done at 500^{o}C. FTIR spectrum indicated the stretching mode of Ti-O bond of a TiO_2. UV–Vis absorption spectra of as-prepared and annealed TiO_2 nanoparticles showed the existence of strong absorption band at low wavelength near 380 nm for anatase and 382 nm for rutile phase respectively. It was clear that the bandgap of the TiO_2 nanoparticles decreased due to increasing temperature.

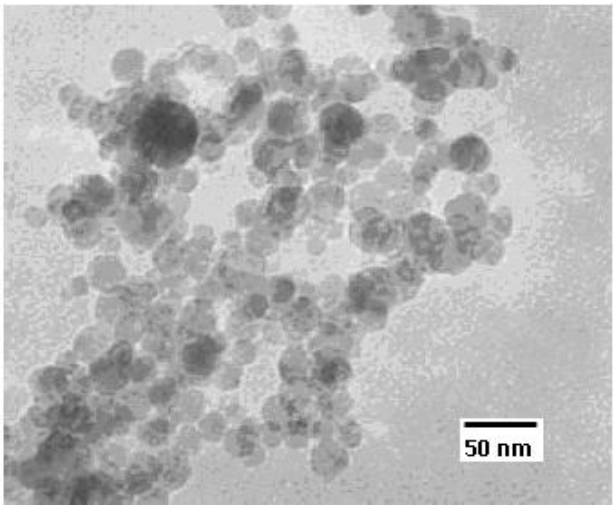

Figure 5. *TEM images of the as-prepared TiO_2 nanoparticles.*

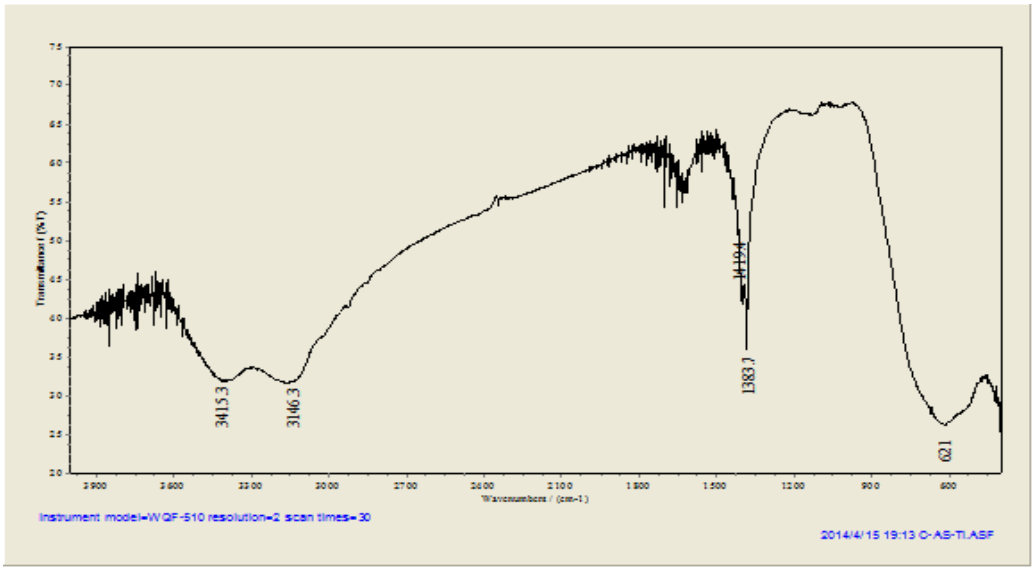

Figure 6. *FTIR spectrum of as-prepared TiO_2 sample.*

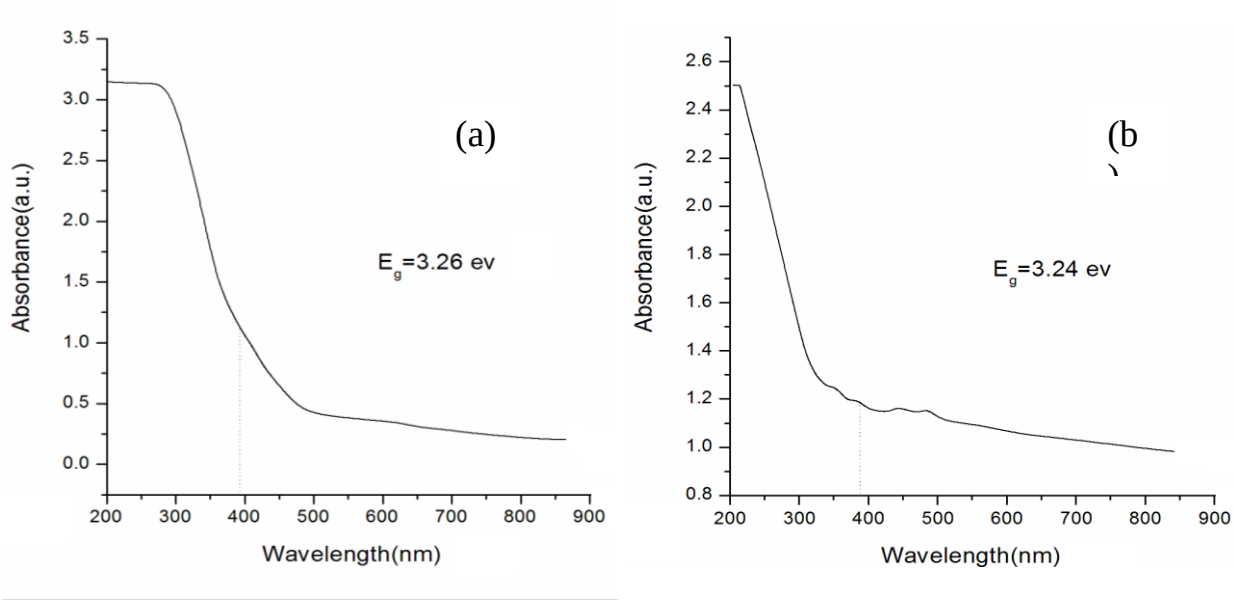

Figure 7. *UV–Vis absorption spectra of (a) as-prepared and (b) annealed TiO_2 nanoparticles.*

ACKNOWLEDGMENTS

The authors are thankful for the financial support of varamin pishva branch at Islamic Azad University for analysis and the discussions on the results.

REFERENCES

1. S.H. Jeong, B.S. Kim, B.T. Lee, H.R. Park and J.K. Kim: J. Korean Phys. Soc. Vol. 41, (2002), pp. 67-72.
2. A.A. Akl, H. Kamal and K. Abdel-Hady: Appl. Surf. Sci. Vol. 252, (2006), pp. 8651–8656.
3. A. Yildiz, S. B. Lisesivdin, M. Kasap and Diana Mardare: J Mater Sci: Mater Electron, Vol. 21, (2010), pp. 692–697
4. W. Li , C. Ni, H. Lin , C. P. Huang and S. Ismat Shah: J. Appl. Phys. Vol. 96, (2004), pp. 6663-6668.
5. E.J. Wolfrum, J. Huang, D.M. Blake, P.C. Maness, Z. Huang, J. Fiest and W.A. Jacoby: Environmental Sci. Tech. Vol. 36 (2002), pp. 3412-3419.
6. J. Jitputti, T. Rattanavoravipa, S. Chuangchote, S. Pavasupree, Y. Suzuki and S. Yoshikawa: Catalysis Communications. Vol. 10, (2009), pp. 378-382.
7. Y. Mizukoshi, Y. Makise, T. Shuto, J. Hu, A. Tominaga, S. Shironita and S. Tanabe: Ultrasonics Sonochem. Vol. 14, (2007), pp. 387-392.
8. Y. Zhanga, H. Zhenga, G. Liub and V. Battagliab: Electrochimica Acta. Vol. 54, (2009), pp- 4079-4083.
9. P.C. Nga, C.S. Denga, M.G. Gub and X.M. Dai: Chem. Phys. Vol. 107, (2008), pp. 77-81.
10. S. Rahim, S. Radiman and A. Hamzah: Sains Malaysiana, Vol. 41, (2012), pp. 219–224.
11. N. Shahruz and H.M. Moghaddam: world appl. Sci. journal, Vol. 12, (2011), pp. 1981-1986.
12. S. Sagadevan: Am. J. Nanosci. Nanotech. Vol. 1, (2013), pp. 27-30.
13. C.H. Lee, S.W. Rhee and H.W. Choi: Nanoscale Res. Lett. Vol. 7, (2012), pp. 48-52.
14. S. Valencia, J. M. Marin and G. Restrepo: Open Mater. Sci. Journal. Vol. 4, (2010), pp. 9-14.
15. N.S. Anwar, A. Kassim, H.L. Lim, S.A. Zakarya and N.M. Huang: Sains Malaysiana. Vol. 39, (2010), pp. 261-265.
16. A. Pottier, C. Chaneac, E. Tronc, L. Mazerolles and J.P. Jolivet: J. Mater. Chem. Vol.11, (2001), pp. 1116-1121.

17. H.A. Monreal, J.G. Chacon-Nava, U. Arce-Colunga, C.A. Martınez, P.G. Casillas and A. Martınez-Villafane: Micro & Nano Letters, Vol. 4, (2009), pp. 187-191.
18. S. Sagadevan: Am. J. Nanosci. Nanotech. Vol.1, (2013), pp. 27-30.
19. Y. Cao, Z. Zhao, J. Yi, C. Ma, D. Zhou, R. Wang, C. Li and J. Qiu: J. Alloys and Compounds. Vol. 554, (2013), pp. 12–20.